ARTICLES

Molecular Beams Studies of the Dissociation of Highly Excited NO_2 Induced by Molecular Colliders

C. R. Bieler,[†] A. Sanov, C. Capellos,[‡] and H. Reisler*

Department of Chemistry, University of Southern California, Los Angeles, California 90089-0482

Received: September 12, 1995; In Final Form: December 1, 1995[⊗]

NO_2 in high vibrational levels was prepared in a pulsed molecular beam by laser excitation of the mixed $1^2A_1/2^2B_2$ state to energies $h\nu$ below dissociation threshold D_0, $D_0 - h\nu = 0-500$ cm^{-1}. The beam of excited molecules was crossed with pulsed, neat molecular beams of HCl, CO_2, N_2O, and NH_3 at relative collision energies of ∼2000 cm^{-1}, and the NO produced by collision-induced dissociation (CID) was detected state-selectively. The CID yield spectra obtained by monitoring specific NO rotational levels while scanning the excitation wavelength show spectral features identical with those in the fluorescence excitation spectrum of NO_2. The yield of the CID products, however, decreases exponentially (compared with the fluorescence spectrum) with the increase of the amount of energy required to reach the threshold of appearance of the monitored NO state. The average energy transferred per activating collision with polyatomic colliders is in the range 130−200 cm^{-1}, having values similar to or lower than those for diatomic and atomic colliders. This is in contrast to deactivating collisions, in which polyatomic colliders are in general more effective. The results are discussed in terms of a mechanism in which the NO_2 molecules are activated by impulsive collisions creating a distribution of molecules in quantum states above D_0 whose populations diminish exponentially with energy. The collisional activation is followed by unimolecular decomposition. The differences between the activation and deactivation pathways are rationalized in terms of the number of degrees of freedom available for energy transfer in each channel.

Introduction

Studies of energy transfer are central to our understanding of unimolecular and bimolecular interactions. In collisional environments and at high temperatures, the high internal and/or translational energies of the colliders eventually lead to dissociation,[1] but collisions of highly internally excited molecules can also lead to relaxation[2−4] and reactions.[5,6] By using molecular beams under single-collision conditions and state-selected laser detection of products, it is now possible to investigate these processes with good energy and quantum-state resolution.

In previous publications, we reported our studies of the collision-induced dissociation (CID) of NO_2 excited to selected energies 0−1000 cm^{-1} below dissociation threshold (D_0 = 25 130 cm^{-1}).[7,8] The NO product was observed state-selectively at relative collision energies 750−2400 cm^{-1}. Our studies with Ar, CO, and O_2 as colliders have demonstrated that when NO_2 is excited to energies just below D_0 CID is rather efficient, but the NO yield decreases in an exponential fashion as the energy, $D_0 - h\nu$, required to reach dissociation threshold increases. The exponential decrease, as well as the NO rotational and spin−orbit distributions, can be rationalized by using a model that separates the collisional activation step from the unimolecular decomposition step. An impulsive collision promotes some of the laser-excited NO_2 molecules, denoted NO_2*, to internal energies above D_0 and these molecules dissociate unimolecularly. The average energy transferred per activating (T → R, V) collision is 100−300 cm^{-1}, and this value depends on the relative collision energy and the nature of the collider. No indication of reactive scattering in collisions with CO and O_2 has been found, despite the fact that the internal energy of NO_2* is sufficient to reach reactive channels yielding CO_2 and O_3, respectively. This latter result is particularly intriguing in light of recent observations that vibrationally excited O_2 molecules with $v \geq 26$ are quenched much more efficiently by O_2 colliders than O_2 with $v < 26$, raising the possibility that for $O_2(v \geq 26)$ the reactive channel yielding O_3 opens up.[9]

In the present article, we extend our studies of the CID of NO_2* to include the molecular colliders HCl, CO_2, N_2O, and NH_3. These studies are motivated in part by recent observations by Hartland and Dai who noted that in the *deactivating* collisions of NO_2*, the average energy transferred per collision is much higher for triatomic colliders, compared with atomic and diatomic colliders.[10,11] It is also known that the quenching rates of NO_2* by molecular colliders such as NH_3 and H_2O are particularly high.[12,13]

A second important issue concerns the influence of attractive forces and reactive pathways in collisions of highly excited molecules. For example, HCl has a permanent dipole moment which may enhance long-range interactions. Also, with HCl and NH_3, reactive channels producing HONO are energetically possible for the high excitation energies of NO_2* used in this study. Would such attractive interactions manifest themselves in the CID channel?

The results obtained in the present work show that the average energy transferred per activating collision with polyatomic colliders is comparable or smaller than that obtained with the

[†] Present address: Department of Chemistry, Albion College, Albion, MI 49224.

[‡] Permanent address: U. S. Army ARDEC, Picatinny Arsenal, AMSTA-AR-AEE, Dover, NJ 07801-5001.

[⊗] Abstract published in *Advance ACS Abstracts,* February 1, 1996.

0022-3654/96/20100-3882$12.00/0

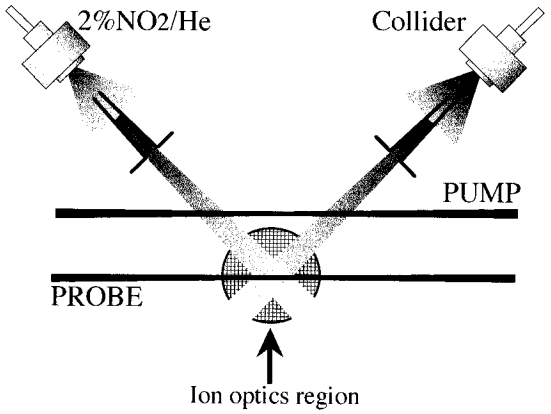

Figure 1. Configuration of the laser and molecular beams used in the CID experiments. The circular area at the intersection of the molecular beams is the ion-optics region of the mass spectrometer mounted perpendicularly to the plane of the molecular and laser beams.

atomic and diatomic colliders studied by us. In addition, no influence of long-range forces could be discerned, suggesting that the probability of inelastic collisions is much larger than that for reactive encounters and/or that the activating collisions are predominantly impulsive at the collision energies used in our studies (1850−2650 cm^{-1}).

Experimental Section

The experiments are performed in a crossed beams apparatus described in detail elsewhere.[8] Briefly, it consists of a main collision chamber and two adjacent molecular beam source chambers. A mixture of 2% NO_2 seeded in He is expanded through a piezoelectrically actuated pulsed nozzle (0.5 mm aperture, ∼150 μs opening time). The mixture is prepared by passing the carrier gas at 1.5−2.0 atm over NO_2 kept at the *o*-xylene/liquid nitrogen slush temperature of −29 °C. A similar nozzle is used for the collider beam in experiments with neat Ar and CO_2, while a General Valve pulsed nozzle (Series 9, 0.5 mm aperture, ∼400 μs opening time) is employed for expansion of neat N_2O, HCl, and NH_3 at a backing pressure of 2.0 atm. The two pulsed molecular beams are differentially pumped and expanded into the interaction chamber through 3 mm diameter homemade skimmers, located ∼50 mm away from the orifice of the NO_2 nozzle and ∼15 mm away from the collider nozzle. The rotational temperature of NO_2 in the molecular beam (3−5 K) is estimated from the rotational distribution of background NO($^2\Pi_{1/2}$) in the NO_2 beam. The vacuum chamber base pressure is $\sim 2 \times 10^{-7}$ Torr, and under typical operating conditions (10 Hz pulse repetition rate, 1.5−2 atm backing pressure) the pressure in the chamber is $\sim 1 \times 10^{-5}$ Torr.

The relative arrangement of the molecular and laser beams in the main collision chamber is shown schematically in Figure 1. The molecular beams travel approximately 50 mm from the skimmer to the center of the chamber and intersect at 90°, creating an overlap region of ∼1 cm^3. Estimates based on the number densities of the NO_2/He and collider beams in the center of the chamber indicate that these experiments are performed under single-collision conditions.[8] The relative NO_2-collider collision energies, estimated for fully expanded beams,[14] are listed in Table 1.

An excimer-laser pumped dye-laser system is utilized for excitation of NO_2 in the molecular beam into mixed $1^2B_2/1^2A_1$ molecular eigenstates, denoted NO_2*. The excitation laser beam (15 ns; ∼5 mJ; 396−414 nm) intersects the NO_2 beam several centimeters away from the skimmer and 20−30 mm before the center of the collision region (see Figure 1). The frequency-doubled output from a second, similar laser system is used as the probe radiation. The probe beam (∼226 nm; 15 ns; ∼150 μJ) crosses the two molecular beams at the center of the collision region. The excitation and probe laser beams are loosely focused with 1 m focal-length lenses to approximately 2 mm and 1 mm spot sizes at their crossings with the molecular beams, respectively, and counterpropagate in the plane of the molecular beams, intersecting them at 45° and 135°.

TABLE 1: Relative Collision Energy and Collisional Energy-Transfer Parameters for NO_2 + M Collision-Induced Dissociation

M	E_{col} (cm^{-1})	γ (cm^{-1})	M	E_{col} (cm^{-1})	γ (cm^{-1})
Ar[a]	2400	307 ± 20	N_2O	2650	158 ± 5
CO[a]	2100	175 ± 8	HCl	2350	150 ± 5
O_2[a]	2200	207 ± 10	NH_3	1850	135 ± 5
CO_2	2600	196 ± 7			

[a] From ref 8.

Exciting NO_2 several centimeters *before* the collision region is crucial for the success of these experiments. Laser excitation must precede collisions to avoid photodissociation following collisional excitation of *ground-state* NO_2.[8] This is achieved by positioning the excitation laser beam upstream, along the NO_2 beam, well outside the molecular beams intersection region (see Figure 1). The 20−30 mm separation between the excitation and probe laser beams requires a 14−20 μs delay between the excitation and probe lasers to allow the NO_2*/He beam to reach the collision/detection region. The long lifetime of NO_2* (∼50 μs)[15] ensures that a significant portion of the NO_2* molecules remain in the excited state upon arrival at the interaction region.

NO is detected state-selectively by resonant multiphoton ionization (REMPI) via the $A^2\Sigma^+ \leftarrow X^2\Pi$ transition using a 1 in. microchannel plate (MCP) detector (Galileo Electro-Optics Corp., FTD2003) located at the end of a home-built Wiley-McLaren time-of-flight (TOF) mass spectrometer,[16] which is mounted above the center of the collision chamber, perpendicular to the plane of the molecular and laser beams. Data processing includes shot-to-shot normalization of the signal using photodiodes (UDT Sensors Inc., UV 1002) to monitor the excitation and probe pulse energies. Due to poor Frank−Condon overlap,[17] the ionization cross section of the A state at 226 nm is much smaller than that for the $A^2\Sigma^+ \leftarrow X^2\Pi$ transition resulting in near saturation of the A ← X transitions at the laser fluences used. Normalization to the probe laser power is performed by assuming total saturation of the main branches of the $A^2\Sigma^+ \leftarrow X^2\Pi$ transition, as confirmed by comparisons with NO spectra obtained at 300 K under similar conditions and results reported elsewhere.[17,18] Although the REMPI intensity is proportional to the number density of the NO molecules, corrections for flux/density transformation were not attempted, since the differences in the *lab* velocities of the detected NO(J) products are relatively small as a result of the high velocities of the molecular beams.

As discussed in detail in a previous publication,[8] several competing processes and background signals must be considered in the data analysis, the most important being signals from background NO, and from NO products obtained via photodissociation of rotationally "hot", ground-state NO_2. First, the signal due to *background* NO in the NO_2 beam (from surface-catalyzed decomposition of NO_2) must be taken into account. Expansion cooling and skimming ensures that the NO background is at $T_{rot} < 5$ K, and only NO molecules in the $^2\Pi_{1/2}$ state with $J \leq 3.5$ have significant population. Nonetheless, in the crossed-beams experiments the background NO in low

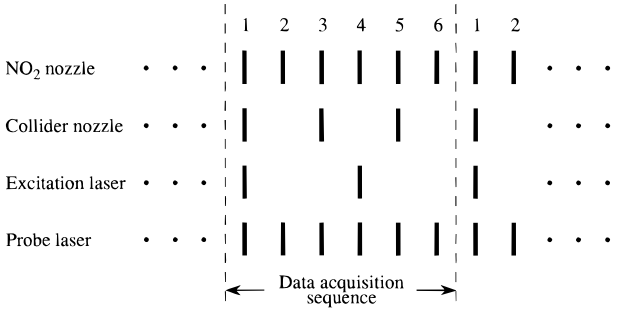

Figure 2. Nozzle and laser firing sequence used in the experiment. Enveloped by the two dashed lines is a single data acquisition loop which includes six firings of the NO_2 nozzle and the probe laser while the collider nozzle and the excitation laser operate in the *on/off* and *on/off/off* regimes, respectively.

rotational states is collisionally scattered into higher-J states,[19,20] and these contributions must be subtracted. Second, we note that even in the absence of collisions with the collider, those NO_2 molecules that are at $N = 2$, 4 in the ≤ 5 K beam will photodissociate when the laser excitation energy is <10 cm^{-1} below D_0. Unlike collisional excitation by the collider beam prior to photoexcitation (see above), this effect cannot be eliminated by moving the pump laser beam away from the collision region. However, this signal is observed only in a small region below D_0 and has been ignored in the analysis of the CID spectra as explained below.

To account for most of the background signals, each data acquisition sequence includes six NO_2 nozzle and probe laser firings, while the collider nozzle is opened only on half of these firings, and the excitation laser is fired on every third pulse of the sequence, as shown schematically in Figure 2. First, with both the excitation laser and collider nozzle *on* (pulse 1 in Figure 2), the CID signal and all the background NO signals are detected by the probe laser. Second, with the excitation laser *on* and the collider nozzle *off* (pulse 4), NO signals from photodissociation of rotationally "warm" NO_2 in the beam are obtained. Third, with the excitation laser *off* and collider nozzle *on* (pulses 3 and 5), NO signals from inelastic scattering of contaminant NO are obtained. Last, NO signals solely due to the unscattered NO background in the NO_2 beam are obtained with both pump laser and collider nozzle *off* (pulses 2 and 6). Subtracting the NO signals obtained with the collider nozzle *off* (pulse 4) from the total signal (pulse 1) yields the collision-induced signal with the excitation laser *on*. Subtracting the average of the NO signals obtained from pulses 3 and 5 of the sequence from that obtained by averaging the signals from pulses 2 and 6 yields the collision induced signal with the excitation laser *off*. Subtracting the latter from the former yields the CID signal, which is typically larger than the background signals by a factor of at least 2. The subtraction of large background signals results in significant uncertainty in the final CID signals, estimated at $\pm 20\%$; however, the shapes of the product state distributions and yield spectra are reproducible.

Results

NO_2 CID yield spectra are obtained by scanning the wavelength of the excitation laser below the NO_2 dissociation threshold, D_0, while monitoring the production of NO ($X^2\Pi_{1/2}$;v=0;J=5.5). Figure 3 shows the CID yield spectra obtained in collisions with CO_2, N_2O, HCl, and NH_3, as a function of the initial excitation energy of NO_2*, $h\nu$. For comparison, the yield spectrum obtained with Ar, which has been previously reported,[8] is also shown. The similarity of all the CID yield spectra is apparent. Each spectrum exhibits

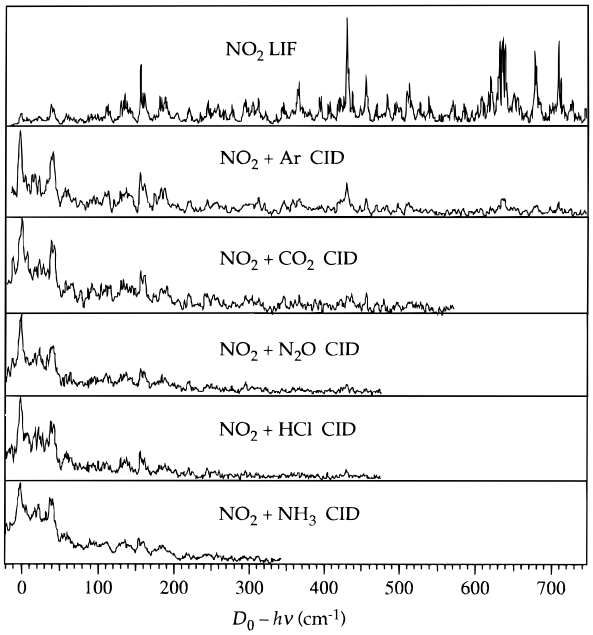

Figure 3. Top: Jet-cooled NO_2 laser-induced fluorescence (LIF) excitation spectrum. Other panels: NO($^2\Pi_{1/2}$;J=5.5) yield from NO_2 CID with different colliders as a function of the initial excitation energy of NO_2.

similar features throughout the wavelength region studied, with the only difference being the relative decrease in CID signal intensity as the excitation laser energy is scanned away from threshold. As previously reported, and confirmed in the present studies, probing different NO product rotational states [e.g., $^2\Pi_{3/2}$(J=5.5,6.5)] results in similar CID yield spectra.[7,8] We also confirm that, as before, the rotational distributions do not depend sensitively on the collider. This observation allows us to extract the relative CID yield by monitoring NO in a single rotational state. The $^2\Pi_{1/2}$(J=5.5) state of NO was chosen, because it is close to the maximum of the typical CID product state distribution,[8] and the fraction of contaminant NO in this level is small.

A key observation in identifying the origin of the NO signal is the structures in the yield spectra. Also shown in Figure 3 is an NO_2 LIF spectrum taken in a companion molecular beam chamber under similar expansion conditions using a GaAs PMT and a filter that transmits fluorescence at 400−900 nm. This wavelength range accounts for the major part of the fluorescence, and since in each experiment the excitation energy is changed by only <20 nm, we do not expect signifcant changes in the fluorescence spectra. The use of the LIF signal as a measure of the relative population in the excitation energy range employed in these experiments is thus justified. As seen from Figure 3, the same structure observed in the LIF spectrum is observed in the CID yield spectra. The fact that the NO yield spectra at $h\nu < D_0$ carry the fingerprints of the NO_2 absorption spectrum is the primary indication that what is observed is in fact CID of photoexcited jet-cooled ($T_{rot} < 5$ K) NO_2. Below D_0, the only significant difference between the NO_2 LIF and CID yield spectra is the relative intensities of the spectral features as the excitation energy $h\nu$ is scanned below D_0. This scaling of the CID yield spectra reflects the decreasing energy transfer efficiency as the amount of energy required to produce NO($^2\Pi_{1/2}$;J=5.5) via CID increases.

To obtain information on the relative efficiency of the collisional activation of laser excited NO_2*, the CID yield spectra shown in Figure 3 must be normalized by the relative NO_2* population as a function of $h\nu$ (i.e., the absorption or LIF

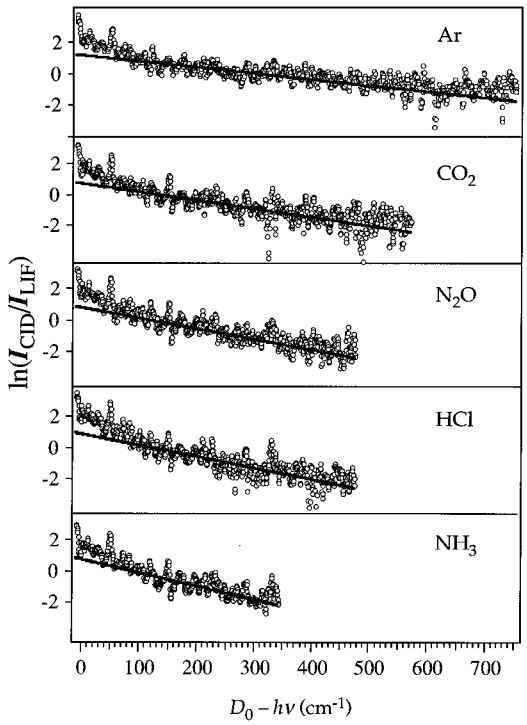

Figure 4. log plots of the point-by-point ratios of the CID yield spectra and the LIF spectrum of NO_2 shown in Figure 3. Solid lines represent the best least-squares fits of the log plots in the energy range 50−460 cm^{-1} below D_0. The slopes of these lines equal the inverse of the energy transfer parameter $1/\gamma$.

spectra of NO_2).[8] Figure 4 presents semi-log plots of the point-by-point ratio of the NO_2 CID and LIF spectra. As discussed in detail previously, the reciprocals of the slopes of $\ln(I_{CID}/I_{LIF})$ *vs* excitation energy curves represent the average energy transferred per activating collision in each system.[8]

The sharp decrease in $\ln(I_{CID}/I_{LIF})$ with decreasing excitation energy just below D_0 (see Figure 4) may in part arise from inelastic scattering of NO generated by photodissociation of rotationally excited NO_2 into the monitored NO(J=5.5). Rotationally excited NO_2 is present in the molecular beam due to both incomplete cooling in the expansion and collisional excitation prior to photoexcitation, which might not be fully eliminated despite the spatial separation of the photoexcitation and collision regions. The contribution of this process can be significant only within several tens of wavenumbers below D_0,[8] and this portion of the spectrum was ignored when analyzing the data. The decay of the normalized CID signal when $h\nu - D_0 > 50$ cm^{-1} is approximately exponential, as indicated by the linearity of the $\ln(I_{CID}/I_{LIF})$ curves. To obtain a quantitative estimate of the average energy transferred per activating collision with the different colliders, least-squares fits of the form $\ln(I_{CID}/I_{LIF}) = a - (D_0 - h\nu)/\gamma$ are used in the range $(D_0 - h\nu) = 50-460$ cm^{-1} to extract the parameter γ for different colliders.[8] The values of γ for all of the colliders studied so far are given in Table 1.

Discussion

The CID yield spectra shown in Figure 3 do not exhibit state-specific effects in the CID of NO_2*; within our signal-to-noise level, the semi-log curves shown in Figure 4 are best described as unstructured, monotonically decaying exponentials. As discussed in a previous publication,[8] the lack of structure in the normalized CID yield spectra is the result of averaging over all activated states of NO_2* whose energies $E^{\ddagger}$ lie above the energy threshold for the monitored NO level. Collisions create a distribution of NO_2 $E^{\ddagger}$ levels above D_0. We assume that the fractional population of each $E^{\ddagger}$ decreases exponentially with $E^{\ddagger}$, and each of these excited NO_2 states decomposes in accordance with statistical theories of unimolecular reactions to produce NO in all the energetically allowed J states. Thus, unlike the photodissociation of NO_2,[21] every NO product state originates from a distribution of NO_2 excess energies.

Since the distribution of collisionally excited NO_2 above D_0 is unknown (the CID signal for any selected NO level is a result of integration over all energetically accessible NO_2* levels with energies above the threshold for the monitored NO product level),[8] no definite conclusion can be drawn about the *state-specific* behavior of the energy-transfer probability. The shape of the $\ln(I_{CID}/I_{LIF})$ spectra in Figure 4 leads us to assume that the probability of collisional excitation decays exponentially with the energy transferred per collision. In addition, in analogy with the photodissociation of NO_2,[21] significant state-to-state fluctuations of the energy transfer cross section may be anticipated. Nonetheless, because of averaging over excited NO_2* states whose energies lie above the threshold of the monitored NO product level, these fluctuations are washed out, as an integrated value does not depend on the exact shape of the state-to-state fluctuations. Thus, we believe that it is justified to deduce the value of the average energy transferred per collision by assuming the exponential decay model.[8]

The reciprocal of the slope of the energy-transfer spectrum defines the average energy transferred per collision, $\langle\Delta E\rangle$, in accordance with the exponential gap law.[22] The energy-transfer parameter γ obtained in the experiments reported here is an average over the range 0−500 cm^{-1} below D_0. This is due to the fact that CID probes only those molecules that are collisionally excited above D_0. In our experiments, detection is at a constant energy while the initial NO_2 excitation energy is varied. The fact that the plots of $\ln(I_{CID}/I_{LIF})$ vs $D_0 - h\nu$ are approximately linear is probably an indication that γ is changing only slightly over this region. In comparing γ for different colliders (Table 1), we find that the average energy transferred per collision is largest for atomic colliders and smallest for polyatomic colliders. Although γ depends also on E_{col}, this fact alone cannot explain the trend observed with these colliders.

The average energy transferred per collision is a measure of the efficiency of collisional excitation or deactivation. By comparing these values for several colliders and comparing results for activating and deactivating collisions, better understanding of the collisional energy transfer process can be obtained. In recent experiments, Dai and co-workers have used a time-resolved Fourier transform emission technique to measure the collisional relaxation of highly excited (∼20 000 cm^{-1}) NO_2* by various colliders under thermal (300 K) conditions.[10,11] The NO_2* energy *loss* per collision with atomic and diatomic colliders (Ar, O_2, CO) is in the range 230−560 cm^{-1}, similar to the average energy transferred per *activating* collision obtained in our NO_2* CID experiments. However, with triatomic colliders, the energy loss per collision is significantly larger than that with the atomic or diatomic colliders (e.g., 1605 and 1127 cm^{-1} for CO_2 and N_2O, respectively). This differs greatly from what is observed in the case of *activating* energy transfer, where triatomic colliders have comparable or smaller T → V, R energy transfer efficiencies than diatomic and atomic collision partners (Table 1). For larger polyatomic colliders, this trend of larger deactivating values (SF_6, toluene)[10,11] and smaller activating values (NH_3) continues.

Similar conclusions regarding deactivation of highly excited NO_2* are reached by comparing the fluorescence quenching rates obtained with different colliders. The quenching rates

depend quite strongly on the level of excitation of NO_2*; in particular, the quenching rates obtained following excitation of NO_2 to levels above the origin of the 1^2B_2 state are substantially higher than those obtained for excitation energies below the origin of this state.[23,24] However, at all excitation energies certain molecular colliders (e.g., CH_2O, NH_3, H_2O) have especially high quenching rates.[12,13]

Several mechanisms may explain the enhanced deactivation rates with molecular colliders. The simplest is based on statistical considerations; as the number of degrees of freedom of the collider increases, more deactivation channels become available. While more V → V, R pathways are opening, the number of T → V, R, channels leading to *activation* of the internal degrees of freedom of NO_2* remains the same, and the balance shifts to deactivation. The initial excitation energy of NO_2 (~20 000 cm^{-1}) is large compared to the collider vibrational quanta, and thus all internal degrees of freedom of the collider, including its vibration, may participate in the energy transfer. In some cases, the available vibrational channels can carry a large amount of the transferred energy. For example, all the vibrational modes of N_2O and CO_2 have been observed to be excited to $v = 1$ in the relaxation of NO_2*.[25,26] Although V → V energy transfer constitutes only a few percent of the total collisions, the higher energies involved [e.g., 2349 cm^{-1} for $CO_2(v_3)$] contribute significantly to the *average* energy transferred per collision.

At the relatively high (compared to thermal) collision energies employed in the experiments reported here, short range, impulsive interactions become dominant.[3] Since the time of an impulsive interaction is quite short, complete energy randomization among all available degrees of freedom of the collision system is not achieved. However, the degrees of freedom of the polyatomic collider may participate to some extent in the energy transfer. For example, when the impact parameter is of the order of the molecular size (as it is for most inelastic collisions), the collider rotation and bending vibrations can be easily activated, absorbing part of the collision energy. In essence, molecular colliders look "softer" to NO_2* due to their vibrational and rotational degrees of freedom, thereby affecting the efficiency of the T → V,R energy transfer to NO_2*.

Although V−V energy transfer is a resonant process and thus may not be efficient with most colliders, the existence of long-range attractive interactions may facilitate the formation of a short-lived complex and thus enhance energy flow to the degrees of freedom of the collider. In such cases, energy will be transferred primarily to the deactivation channels. Several investigators have suggested that the strength of the long-range interactions in NO_2 may be influenced by the availability of low-lying electronic states.[10,23] Hartland et al.[10] propose that due to vibronic coupling between the NO_2 excited $^2B_2$ and ground $^2A_1$ states, the electronic dipole moment contributes to the collisional energy transfer. This may contribute to the enhanced quenching rates with specific molecular colliders. In this regard, NO_2 with its low-lying electronic states may be a special case.

We point out, however, that because of the significant difference in experimental conditions between our molecular beam experiments and the thermal relaxation measurements of NO_2*, quantitative comparisons cannot be made. In the thermal experiments the relative collision energies have a wide distribution peaking around 200 cm^{-1} (300 K), whereas the experiments reported here are performed with well-defined collision energies which are ~10 times larger than the average thermal collision energy. As has been shown previously, the γ parameter depends markedly on translational energy.[8] At low collision energies long-range mechanisms such as dipole−dipole coupling are important for V−V transfer,[26] but the effects of long-range forces may become less important with increasing collision energy.

Finally, we would like to comment on the probability of reactive channels in collisions of highly excited NO_2. In fact, several of the colliders in our studies were chosen because of their possible reactivity with NO_2*. CO and O_2 can yield NO as a product, while HCl and NH_3 can give HONO. Nevertheless, no indication of the existence of reactive pathways has been obtained. Especially intriguing is the possibility of the reaction $NO_2^* + O_2 \rightarrow NO + O_3$ which has atmospheric implications. The reverse reaction is known to produce NO_2*,[27,28] and thus one might expect vibrational excitation in NO_2 to enhance reactivity. Several reasons may contribute to our inability to observe effects due to reaction. First, due to the existence of background NO in our experiments, the inherent low S/N prevents us from identifying a small contribution from a chemical reaction that will manifest itself as a deviation from the exponential decay law. Second, the reverse reaction is thought to proceed mainly on the ground electronic PES and produces NO_2* with much lower levels of excitation than those employed in our study.[28] Thus, the enhanced excitation of NO_2* will not necessarily lead to higher reaction probability. A third consideration, and probably the most general one, is that inelastic scattering may have fewer geometrical constraints compared to an approach leading to reaction, and therefore even if by statistical considerations alone the observation of a reactive channel is feasible, steric effects may reduce the contribution of reactive pathways even further. It should also be recognized that not all vibrational motions are equally effective in coupling to the reaction coordinate and promoting reactivity. In this regard, a diatomic reactant such as vibrationally excited O_2 (which has only one vibrational mode) may exhibit a higher probability for reaction than a polyatomic collider with a comparable level of excitation.

The probability of the reaction of NO_2* with CO, which has an activation energy of 11 050 cm^{-1}, is known to be low. Bulk 300 K experiments have yielded a reaction probability 2−3 orders of magnitude smaller than the NO_2* quenching probability.[29,30] By microscopic reversibility, the latter should have the same order of magnitude as the CID probability at excitation energies just below D_0. It is clear that the increased translational energy available in our experiments does not increase this probability significantly. For the other polyatomic colliders studied here, the reverse reactions have not been investigated, and no other products were searched for. Thus, we can only speculate that since their yield spectra appear similar to those of the atomic and diatomic colliders, their reaction probabilites are low under our experimental conditions.

Summary

Gas-phase CID of highly excited NO_2* has been studied with different polyatomic colliders at well-defined hyperthermal collision energies. CID can be described as a two-step process. The first step involves collisional activation of NO_2*, in which a distribution of NO_2* molecules with energies above D_0 is created. This is followed by unimolecular decomposition to yield NO + O, in which the collider plays mostly a spectator role.[8] Although the intermediate distribution of collisionally excited NO_2* above D_0 cannot be measured in our experiments, indications about its form are derived from the CID yield spectra and NO product-state distributions. A statistical model based on the assumption that the fractional population of NO_2* above D_0 decreases exponentially with increasing energy reproduces the experimental observations.[8]

At the collision energies employed in the present experiments, $E_{col} \sim 2000$ cm^{-1}, the activating collisions are predominantly impulsive, i.e., the short-range repulsive wall of the potential plays the main role, while the effects of long-range chemical interactions are insignificant. This conclusion is supported by the observation that for all the studied colliders, the CID yield spectra appear rather similar.

We also observe that the average energy transferred per activating collision decreases with the level of complexity of the collider (i.e., γ is larger for Ar than for CO_2, N_2O, and NH_3). It is possible that the greater efficacy of T → V,R transfer involving internal degrees of freedom of the molecular colliders competes with conversion of translational energy to NO_2* internal energy. Independent experiments show that in thermal environments both the average energy transferred per deactivating collision and the quenching rate of NO_2* increase with increasing complexity of the collider.

One of the goals of these experiments was to assess the contribution of reactive channels in collisions of highly excited NO_2*, particularly with HCl and NH_3. However, no signatures of reactions are observed in the present experiments, as well as in collisions with CO and O_2.[8] In all cases, the CID yield spectra are very similar to the spectrum observed when Ar is the collider and no reaction is possible. It is thus concluded that CID is the predominant channel at the collision and excitation energies employed in our experiments.

Acknowledgment. The authors wish to thank the U.S. Army Research Office and the National Science Foundation for supporting this research.

References and Notes

(1) (a) Forst, W. *Theory of Unimolecular Reactions*; Academic: New York, 1973. (b) Robinson, P. J.; Holbrook, K. A. *Unimolecular Reactions*; Wiley: New York, 1972. (c) Gilbert, R. G.; Smith, S. C. *Theory of Unimolecular and Recombination Reactions*; Blackwell Scientific: Oxford, 1990.

(2) Hippler, H.; Troe, J. In *Bimolecular Collisions*; Bagott, J. E., Ashfold, M. N. R., Eds.; The Royal Society of Chemistry: London, 1989.

(3) Flynn, G. W.; Weston, R. E., Jr. *J. Phys. Chem.* **1993**, *97*, 8116.

(4) Yardley, J. T. *Introduction to Molecular Energy Transfer*; Academic Press: New York, 1980.

(5) Tardy, D. C.; Rabinovitch, B. S. *Chem. Rev.* **1977**, *77*, 396.

(6) (a) Metz, R. B.; Pfeiffer, J. M.; Thoemke, J. D.; Crim, F. F. *Chem. Phys. Lett.* **1994**, *221*, 347. (b) Metz, R. B.; Thoemke, J. D.; Pfeiffer, J. M.; Crim, F. F. *J. Chem. Phys.* **1993**, *99*, 1744. (c) Sinha, A.; Thoemke, J. D.; Crim, F. F., *J. Chem. Phys.* **1992**, *96*, 372. (d) Sinha, A.; Hsiao, M. C.; Crim, F. F. *J. Chem. Phys.* **1991**, *94*, 4928.

(7) Bieler, C. R.; Sanov, A.; Hunter, M.; Reisler, H. *J. Phys. Chem.* **1994**, *98*, 1058.

(8) Sanov, A.; Bieler, C. R.; Reisler, H. *J. Phys. Chem.* **1995**, *99*, 7339.

(9) Miller, R. L.; Suits, A. G.; Houston, P. L.; Toumi, R.; Mack, J. A.; Wodtke, A. M. *Science* **1994**, *265*, 1831.

(10) Hartland, G. V.; Qin, D.; Dai, H.-L. *J. Chem. Phys.* **1995**, *102*, 8677.

(11) Hatland, G. V.; Dai, H.-L., private communication.

(12) Donnelly, V. M.; Keil, D. G.; Kaufman, F. *J. Chem. Phys.* **1979**, *71*, 659.

(13) Capellos, C. *Proceedings of the Army Science Conference*; Orlando, FL, 1994; Assistant Secretary of the Army, Office of the Director of Research, Development and Acquisition, Contract number DAAH04-93-C10048; Vol. 1, pp 51−58.

(14) Kolodney, E.; Amirav, A. *Chem. Phys.* **1983**, *82*, 269.

(15) Patten, Jr., K. O.; Burley, J. D.; Johnston, H. S. *J. Phys. Chem.* **1990**, *94*, 7960.

(16) Wiley, W. C.; McLaren, I. H. *Rev. Sci. Instrum.* **1955**, *26*, 1150.

(17) Miller, J. C.; Compton, R. N. *Chem. Phys.* **1981**, *75*, 22.

(18) Jacobs, D. C.; Zare, R. N. *J. Chem. Phys.* **1986**, *85*, 5457.

(19) Joswig, H.; Andresen, P.; Schinke, R. *J. Chem. Phys.* **1986**, *85*, 1904.

(20) Bieler, C. R.; Sanov, A.; Reisler, H. *Chem. Phys. Lett.* **1995**, *235*, 175.

(21) (a) Hunter, M.; Reid, S. A.; Robie, D. C.; Reisler, H. *J. Chem. Phys.* **1993**, *99*, 1093. (b) Reid, S. A.; Robie, D. C.; Reisler, H. *J. Chem. Phys.* **1994**, *100*, 4256.

(22) Troe, J. *J. Chem. Phys.* **1977**, *66*, 4745.

(23) Toselli, B. M.; Walunas, T. L.; Barker, J. R. *J. Chem. Phys.* **1990**, *92*, 4793.

(24) Hartland, G. V.; Qin, D.; Dai, H.-L. *J. Chem. Phys.* **1994**, *100*, 7832.

(25) Chou, J. Z.; Hewitt, S. A.; Hershberger, J. F.; Flynn, G. W. *J. Chem. Phys.* **1990**, *93*, 8474.

(26) Hartland, G. V.; Qin, D.; Dai, H.-L. *J. Chem. Phys.* **1994**, *101*, 8554.

(27) Kahler, C. C.; Ansell, E.; Upshur, C. M.; Green, Jr., W. H. *J. Chem. Phys.* **1984**, *80*, 3644.

(28) Redpath, A. E.; Menzinger, M.; Carrington, T. *Chem. Phys.* **1978**, *27*, 409.

(29) Herman, I. P.; Mariella, Jr., R. P.; Javan, A. *J. Chem. Phys.* **1978**, *68*, 1070.

(30) Umstead, M. E.; Lloyd, S. A.; Lin, M. C. *Appl. Phys. B* **1986**, *39*, 55.

JP952663M